SPE 99352

An Efficient Model for Gas-Rate Forecasting in Complex Reservoirs

C.L. Jordan, M.J. Fenniak, and C.R. Smith, Rapid Technology Corp.

This paper was prepared for presentation at the 2006 SPE Gas Technology Symposium held in Calgary, Alberta, Canada, 15–17 May 2006.

Abstract

This paper presents a simple, but accurate, computer method for predicting the performance of multiple gas wells in complex reservoir scenarios. Real life gas reservoir characterization and forecasting can be accomplished with the substantial reduction of effort when compared to numerical simulation and a substantial increase in accuracy when compared to traditional decline methods. Conventional analytical methods in many cases are highly unsuitable for new field development, in-fill drilling, or long-term production planning. Numerical simulation methods often require impractical pre-processing or computational time. With the method presented in this paper, production profiles can be generated for arbitrary shaped gas reservoirs with multiple wells. The model presented overcomes many limitations of traditional methods, and extends analytical modeling into multiple well scenarios with interference effects, arbitrary reservoir shapes, and perhaps even varying rock properties.

Introduction: General History & Motiviation

Modeling of petroleum reservoirs and its application to pressure and production analysis have been studied for years. Publications by Hurst (1981), Lee (1982), Streltsova (1988), Stanislav and Kabir (1990), Raghavan (1993), Mattox and Dalton (1990), and Settari and Aziz (1979) cover the important concepts of both numerical and analytical models. Others such as Muskat (1937) and Van Everdingen and Hurst (1949) outline more specific solutions for constant rate drawdown in infinite reservoirs, while Matthews, Brons, and Hazerbroek (1954) and Dietz (1965) investigated solutions for a single well in a bounded reservoir. Agarwal, Al-Hussainy and Ramey (1970) included wellbore storage and skin effects into the wellbore boundary conditions. Odeh and Jones (1965) described the pressure changes due to variable rate production. The list of contributors to the science and technology of reservoir modeling is extensive – and can generally be classified into either analytical or numerical.

With respect to analytical methods, there are only a few conventional methods for solving the diffusivity equation. These include separation of variables, eigenfunction expansion, similarity transform, Laplace Transform, Fourier Transform, and Green's functions. However, due to certain restrictions in solving such problems, analytic methods are generally only amendable to simple geometric shapes. Generally, this problem can be alleviated by superposition (assuming linear differential operators).

The shortcomings of analytical methods are also alleviated by numerical schemes such as the Finite Element Method (FEM) and Finite Difference Method (FDM) which have a greater flexibility in solving complex problems – however, this is generally at the expense of time and computational power. For example, with FEM, users must spend significant amounts of time generating appropriate grid orientation, and ensuring that accuracy is not compromised due to numerical dispersion etc. A literature review suggested that a good comparison of FDM and FEM is given by Russell and Wheeler.

Therefore, a technique which has the accuracy of the analytical methods and preserves the versatility of the numerical techniques to solve complex reservoir problems is highly desirable. As a result, the Boundary Element Method (BEM) has become popular, and has been heavily studied by Kikani[1], Archer[2], and Pecher[3] to name a few. Others such as Larsen attempted to improve the use of superposition to handle more complicated reservoir geometry. In all cases, significant computation effort was required for success – either in calculating image well locations or evaluating complex (and sometimes undefined) integrals. Lin[4], Caudle[5], Jankovic[6], and Haitjema[7] made use of approximate forms of superposition to handle more sophisticated aspects of multi-well interaction – however, most studies were limited to steady state applications for pressure contour and streamline mapping.

The objective of this paper is provide a simple method for calculating pressure and rate profiles for multiple wells within an arbitrary shaped reservoir, solely using approximate superposition methods, eliminating the overhead due to calculating exact image well placement. As a result, the proposed method would maintain the appeal of BEM, but eliminate the need for evaluating complex functions, and yet be far more versatile than simple geometric solutions. Furthermore, by incorporating modern concepts such as real

gas flow, the proposed solution would be suitable for accurate gas pressure-production forecasting during both the transient and boundary dominated flow regimes.

Paper Organization

For convenience and clarity, this paper is to be broken into four major sections as outlined below. Each section qualitatively describes the relative problems and solutions with reference to appropriate appendix for further details.

1) Theory:
   - Theory 1: Standard Superposition
   - Theory 2: PSS for Arbitrary Shape
   - Theory 3: Transient Flow in Arbitrary Shape
   - Theory 4: Laplace Space Formulation
   - Theory 5: De-superposition
   - Theory 6: Real Gas Flow Considerations
   - Theory 7: Rate & Pressure Forecasting.
2) Summary of Solution Process
3) Testing & Verification
4) Conclusions & Future Work

Theory

Theory 1: Standard Superposition. The fact that most continuity equations developed for fluid flow in porous media applications are linear[8] permits the use of a powerful tool – the principle of superposition. The principle of superposition means the presence of one boundary condition does not affect the response produced by the presence of other boundary or initial conditions, and that there are no interactions among the responses produced by the different boundary conditions. Therefore, to analyze the combined effect of a number of boundary conditions, we may start by solving for the effect of each individual condition and then combine the results[8].

For example, we commonly solve the diffusivity equation for the conditions of a single well producing at a constant rate in an infinite reservoir. If we superimpose the same solution at another coordinate in the reservoir, then one gets a single no-flow boundary condition between the two wells. It has also been demonstrated that single well solutions can be superimposed to generate the behavior of bounded geometric shapes (i.e. a rectangular reservoir) by adding together the pressure disturbances caused by an appropriate array of an infinite number of wells producing in an infinite system (commonly referred to as image wells) [9,10,11,12]. As a result, without any consideration to varying rate schedule or multiple wells, generating a suitable solution for a single well in somewhat irregular shaped reservoir (for example, a four sided polygon, or a well located within a wedge) becomes a fairly tedious task due to calculating the large number of image wells (and their respective positions) required to approximate the infinite summation. In order to alleviate the problems associated with approximating reservoir boundaries in complex geometries with a finite series of image wells, the modeling process in this paper relied upon a methodology first introduced by Caudle, Jankovic, Lin, and others [4,5,6].

Theory 2: PSS for Arbitrary Shape. The solutions published by Caudle, Jankovic, Lin, and others [4,5,6], in the context of steady-state or pseudo-steady state (PSS) problems, were to approximate a large (but finite) number of correctly positioned image wells with less than 60 "pseudo" image wells located at along the perimeter of the arbitrary shape. In all cases, the flow rates of the pseudo image wells were determined such that an equal potential existed at a number of collocation or test points along the boundary. Basically, the normal potential was evaluated at a number of test points located along the boundary to ensure that difference was zero across the boundary (the objective was to achieve a Neumann boundary condition). All the work presented by the authors of this paper will focus entirely on creating no-flow boundary conditions, although the method can be applied to constant pressure or other boundary conditions.

Haitjema[7] and Jankovic[6], who did extensive work in hydrology, found that in a number of cases the errors between test points can become large and resulting solutions unacceptable. Increasing the number of test points only increased the error. As a result, rather than meeting the desired boundary conditions exactly at the test points, an average solution was introduced by having more test points than pseudo image wells. This resulted in a least squares solution in which the boundary condition is met along the entire boundary in an average sense. In some instances, a singular value decomposition[13] approach was used to overcome ill-conditioned matrices. Experimentation from various authors has shown that a 2:1 ratio of test points to pseudo image wells is close to ideal[5]. For the work presented in this paper, 36 pseudo image wells and 72 test points were used for all examples presented. All pseudo image wells were placed twice the average boundary distance from the center of the reservoir (refer to Figure 1).

This technique proved to be very efficient computationally as one could arbitrarily pick the locations and adjust the constants (i.e. power and strength) of these image wells so that the boundary conditions are met. Since the solution only honors the desired boundary condition at a number of test points along the boundary, the solution is approximate. Nevertheless, this method gave good bounding for steady-state flow systems, and has been heavily used to date in the hydrology industry.

The theoretical justification of such work is nicely summed up by Bear[8] who stated that any linear combination of solutions to a linear partial differential equation is also a solution to that same PDE. In other words, If p_{D1}, p_{D2},… p_{Dn} are individual solutions to the diffusivity equation, then $C_1 \times p_{D1} + C_2 \times p_{D2} + .. C_n \times p_{Dn}$ is also a solution where C_1, C_2 … C_n are arbitrary constants adjusted such that the new desired boundary conditions are satisfied (refer to Appendix 1). In the case of true mirror image wells, the constants are unity due to the perfect choice of image well position. The next section describes its application to both transient and PSS flow periods.

Incidentally, Guevara-Jordan[13] *et al* made use of this approach for multiple wells in a sectionally homogeneous reservoir (his work indicated that approximately 54 pseudo-image wells, 64 test points produced suitable solutions). Similar to the previous work done in this area, Guevara-

Jordan[14] *et al* focused primarily on streamline mapping during PSS. Rate and pressure forecasting was not addressed in his work.

Theory 3: Transient Flow in Arbitrary Shape. For transient (or unsteady) problems, the conventional techniques of creating boundaries have been limited to symmetric shapes, while solutions for bounding of irregular areas have been more elusive. The work in the previous section was later followed by Hong-Chen[14] who adapted the procedure to unsteady-state flow.

Hong-Chen[14] concluded that a) a single ring of pseudo image wells was sufficient to bound a reservoir, b) that the strength of these pseudo image wells needed to be taken into account in the superposition algorithm for accurate typecurve generation, c) without the superposition effect of pseudo image wells, the solution was only sufficient for streamline generation, and d) the number of pseudo image wells should be in the range of 20 to 30 with twice as many bounding points. Other observations were that the time-stepping used in the typecurve generation procedure was critical. The results showed that the size of dimensionless time increment should be in the range of 0.06 – 0.018, which is impractical for the typical time domains associated with PSS.

The time steps (and associated rate superposition for the pseudo image wells) required to make a smooth transition from transient to PSS flow was found to be impractical for day-to-day use (even before the introduction of real gas flow etc). This cumbersome procedure had to be continually repeated for each well before the various typecurves could be superimposed to create a multiple well reservoir. In order to alleviate the problem of computation speed, the solution process was adapted to Laplace Space as discussed in the next section of this paper.

Incidentally, Britto[15] *et al* did publish work describing how to introduce an impermeable region near a well located within an infinite reservoir. Generally, Hong-Chen[14], Britto[15] *et al*, and others doing similar work only applied this technology to pressure transient analysis (i.e. constant rate typecurve generation), or streamline generation. No work focused on complex well production forecasting and/or reservoir characterization.

Theory 4: Laplace Space Formulation. In order to alleviate the problem of large computational calculations discussed in the previous section, the solution process was performed in Laplace space. The advantage that can be anticipated is that time appears as a parameter in Laplace space thereby removing the complication arising from rate superposition[1]. Another advantage, pointed out by Pecher[16], is that since the solution at a given time is not dependant on the solutions at previous times, there is no accumulation of error for longer solution times. As a result, the strengths of the pseudo image wells can be solved at any point in time without having to consider problems associated time stepping and rate superposition – only space superposition needed to be considered. Appendix 2 shows the Laplace space Green's function for a cylindrical source in an infinite medium and while Appendix 3 shows the associated normal derivatives for the same function.

The only significant drawback of the Laplace transform technique is the need for an inversion method of the solution back to the real-time space. Inversion can be accomplished by using tables of integral transforms, such as Erdelyi's, or by applying what is commonly know as the complex inversion formula[17]. In the context of BEM, many have used Schapery's method[16]. Another method known as the Stefhest algorithm[18] (Appendix 5) is a method for approximate, numerical inversion of Laplace Transforms. It is widely used in petroleum engineering, and is generally amenable to computer calculation[17]. However, Stefhest's method suffered from some numerical instability problems for the solution presented in this paper.

As a result, an approximate solution, hailed as the Bourgeous method[19] in this paper, allowed for the inversion of laplace solutions by simply using $p_D(t_D)=p_D(s)\times(s)$ where $s = 1/t_D$, and t_D is the time of interest. In his original work, Bourgeous did not directly claim that this aforementioned calculation could be used to invert Laplace solutions. However, he did show that the asymptotes (i.e. the radial flow time period) of Laplace and real space solutions for a vertical well, fully completed, in a homogeneous infinite-acting reservoir were nearly equivalent (refer to Appendix 6). Figure 2 shows the inversion of the solution for a single well in closed reservoir using both Stefhest and the proposed Bourgeous method. A review of the Figure 2 indicates that approximation is suitable. Similar approaches have been proposed by other authors using Laplace space transformations in CBM applications, but were found not to be satisfactory.

During the solution process, the rate at the single real well was always assumed to be constant and unity, therefore the final generated typecurve for the well is a constant rate typecurve for a single well in a bounded arbitrarily shaped reservoir. Conventional superposition will be used to generate the pressure and/or production behavior for multiple wells in the reservoir. The approximate superposition method presented in earlier sections was only used for the single well typecurve.

Theory 5: De-superposition. Others including Gringarten, Ramey, and Raghavan[20] as well as Chen and Brigham[21] have illustrated the concept of de-superposition for modifying known p_D values to p_D's for somewhat different systems. The approach may be used for any drainage shape and well location, and is well illustrated and documented in the classic PTA papers [20,21,22].

Suppose one can compute the pressure behavior, p_D, for a well located in the center of square without wellbore storage ($c_D = 0$). One can then compute the pressure disturbance for the same system with wellbore storage by simply removing (subtracting) the solution for a single well in an infinite system and then adding the solution for well, including wellbore storage, in an infinite system. Gringarten, Ramey, and Raghaven[20] used this approach to estimate dimensionless pressure for closed fractured systems. Similarly, Chen and Brigham[21] used this approach to generate dimensionless pressures for a single well with wellbore storage and skin in the center of a closed square. Likewise, the authors of this paper will use this approach to add wellbore storage, dual

porosity, skin, and even a hydraulic fracture to solutions generated for a single well in an arbitrary shaped reservoir. Figure 3 shows the typecurves for a single well in a bounded system prior to, and after the addition of dual porosity using de-superposition. Boundary effects were added only to the original typecurve using the pseudo-image well method.

Theory 6: Rate & Pressure Forecasting. Once the real space typecurves have been generated for each individual well in the real system, pressure profiles can be easily generated for each well in the system using conventional superposition assuming well rates are known. Appendix 7 outlines the common calculation procedure for calculating the pressure response of multiple wells with varying rate history. For rate forecasting, the problem becomes a little more complex. Specifically, the superposition algorithm presented in Appendix 7 must be re-arranged for the final time step in which the rates are unknown – however, since the rate of any well of interest is influenced by rate of all other wells in the system, a matrix problem occurs. Luckily, the matrix is always a square matrix, and simple matrix operations can be utilized to solve for unknown rates. Appendix 8 summarizes the calculations necessary to generate a rate forecast.

Theory 7: Real Gas Flow. It is well know that gas properties are non-linear with respect to pressure. In order to add the non-linear behavior of gas to the solution (termed real gas flow in this paper) the concepts of pseudo-time and pseudo-pressure are used. The concept of pseudo-pressure (sometimes called the real gas potential), which handles variable viscosity, and compressibility factor (μZ) is well known and was documented as early as the mid 70's by Al-Hussainy and Ramey [11,23,24,26]. The transformation of pressure to pseudo-pressure is exact, and completely rigorous although it is evaluated numerically. Appendix 10 shows the pseudo-pressure definition.

The concept of pseudo-time which handles variable viscosity and compressibility (μC_t) was, until recently, not amendable to a completely rigorous solution[24]. Rahaman[27] *et al*, introduced a new method for computing pseudo-time based upon material balance. This pseudo-time introduced by Rahaman[27] *et al* was primarily used for improving the forecasting of gas production when significant depletion was observed – gas properties are conceptually evaluated at average reservoir pressure during the life of the well. This is different than the pseudo-time introduced by Agarwal[28] in 1980 which focused on the pressure regime in wellbores and was used to correct the non-linear behavior of gas during buildups. Without introducing pseudo-time, gas rate forecasting using the traditional assumption of constant compressibility under-predicts the recoverable reserves (Figure 4). The pseudo-time formulation has corrected this problem and has significantly improved the quality of long-term forecasting of gas production.

The addition of pseudo-time to this paper does present some basic problems. Specifically, the pseudo-time formulation presented in Appendix 9 requires that one knows the gas rate at time "t" – this, of course, poses a problem when predicting or forecasting gas rates. As a result, the forecast solution becomes iterative. Specifically, the solution requires that the rate prediction initially be done with assuming normal time. The second iteration is then done using pseudo-time based on the previously calculated gas rates. Originally, convergence criteria on both gas rates and pseudo-time itself were incorporated in the solution process, however, extensive testing showed that five iterations is sufficient for most production forecasts. For the work presented here, pseudo-time is based upon the total pool gas rate if multiple wells are producing in the reservoir.

Solution Process

Given the theory outlined in the previous sections, the rate pressure profile for multiple wells in an arbitrary shaped reservoir can be generated by:

1) For each well:
    a. Using the Laplace Space formulation of the problem, solve for the pseudo image well strengths by solving the matrix calculations as shown in Appendix 4.
    b. Convert the typecurve to the real space formulation of the problem using $p_D(t_D)=p_D(s)\times(s)$ where $s = 1/t_D$.
    c. Use de-superposition to add wellbore storage, fracture parameters, etc. to the existing typecurves.
2) Use conventional superposition-in-space when generating the rate-pressure response for multiple wells within the bounded reservoir.
3) Use conventional superposition-in-time to generate multi-rate scenarios for each well.
    a. When evaluating wellbore pressure for known rates, generate a) pseudo-time for the given rate history, and b) a pseudo-pressure table from known fluid properties. Convert pseudo-time to dimensionless time (t_{Da}), and lookup dimensionless pressure (p_D). Using pseudo-pressure table, convert dimensionless pressure (p_D) to pseudo-pressure, and then convert pseudo-pressure to real wellbore pressures (p_{wf}) using previously generated table.
    b. When evaluating rates for known wellbore pressure history, a) generate pseudo-pressure table from known fluid properties. Convert pseudo-pressures to dimensionless pressure (p_D), and back calculate "q" for desired dimensionless real time (t_D). Calculate new pseudo-time t_{Da} based on q, and repeat procedure until q and t_{Da} convergence.

All dimensionless variable definitions used in the solution process are shown in Appendix 12.

Verification Methods

A variety of methods were used to verify the new reservoir model.

1) As all cases were conducted with a closed reservoir, correct reserves (and therefore no violation of the no-flow boundary) could be easily verified. A pseudo-steady state

typecurve (see Appendix 11) was generated based upon the known initial gas-in-place and was compared with an individual well's typecurve. Although not shown, the PSS typecurve can be derived by taking the late time asymptote of van Everdingen and Hurst's[29] constant rate solution for a well located with the center of the circular reservoir.

2) Some cases contained simple reservoir shapes, such as a single well in the center of a circular reservoir. In these cases, well-known analytical models could be used as a basis for comparison [9,20,22,26].

3) A variety of cases with multiple wells were symmetrical. The multiple-well model would then create no-flow boundaries that isolated each well. Pressure or rate forecasts were then generated with single-well models for comparison. Matthews and Russell[22] as well as Mattews, Brons, and Hazebroek[30], extensively researched this phenomenon and showed that typecurves for a multi well system would be identical if wells produced at equal rates, and were located with symmetry with respect to the boundaries and each other.

4) Numerical simulation methods were used to generate comparable cases for some of the more complex reservoirs. The numerical simulator used was based upon a unstructured (Voroni) grid generation technique, allowing it to easily use reservoir geometry identical to our model without manually creating simulation grids.

5) Advanced production data analysis (PDA) techniques (see Appendix 11) were used on pressure and rate forecasts as another check to verify that reserves were honored by the model. These include methods published by Argarwal and Gardner[31], and Wattenbarger[32] *et al*, all who sought to linearize gas production data during PSS such that OGIP could be determined. In all cases, the authors took into account the impact of pressure dependant gas properties.

Verification Case 1: Multiple Wells. To show that the forecast technique works for multiple wells, a symmetrical case was developed. A two-mile by two-mile square reservoir was used. Four wells are placed in the reservoir, each in the center of a one-square-mile corner of the square. Each well would be produced with identical gas rates. The reservoir model will be verified as successful if all four wells show an identical pressure response. Additionally, the model results should compare very closely with a single well simulation configured with one-quarter of the drainage area. Typecurve comparison with a numerical simulator was performed as well [33,34,35,36].

Common reservoir properties (as described in Table 1) were used to create this model. The reservoir geometry is shown in Figure 5. This reservoir had an initial gas-in-place of 35.4 Bcf. All four wells in the reservoir model produced at a constant rate of 5 Mmscf/d for a period of 8766 hours (approximately one year), producing a total of 7.31 Bcf. Sandface pressures were calculated at 100 logarithmically spaced points.

All four wells in the reservoir model calculated nearly identical sandface pressures. Figure 8 shows the "Single-Well" model was very similar to any well from the original pressure forecast, with a slight difference of 13 psi (0.3% of initial reservoir pressure). This suggests that a no-flow boundary is forming half-way between each well, isolating each well into an identical one-square-mile drainage area.

For further verification, the analytical constant rate solution by Earlougher [10] *et al* for a single well located within the center of a rectangle was also generated – but for a square reservoir with ¼ of the size presented in Figure 5 (i.e. 8.85 Bcf), and with the well located centrally. Then the raw data for a single well was converted to dimensionless values and placed on the same plot. Figure 6 shows that both models match closely. As pointed out by Matthews and Russell[22] as well as Mattews, Brons, and Hazebroek[30], pressure behavior a single well in a pure symmetry case should be equivalent to a single well in a smaller reservoir with an area of A/(Number of Wells). This indicates that both a) the generation of the outer boundaries is reliable, and b) the conventional superposition method for multiwell interaction is reliable.

Figure 7 shows the dimensionless typecurves for a single well (prior to multi well interaction) with the boundaries associated with Figure 5, using both the Voronoi simulator, and the new proposed method. As can be seen, both methods compare well with transient as well PSS behavior. The PSS derivative is denoted as the "reserves" line in Figure 7, and other plots.

Modern PDA techniques[31,32] were used on the pressure simulation of one well. The normalized decline analysis, based on methods outlined in Appendix 11, showed nearly identical reserves (8.53 Bcf) and permeability (10.2 md). This indicates that the new model is suitable for long-term deliverability forecasting, and that we are honoring the real gas physics. As implied in Figure 4, if pseudo-time and pseudo-pressure had not been incorporated correctly into the proposed model, normalized decline would report a lower OGIP.

Verification Case 2: Complex Shape. A reservoir shape resembling an "X" was one of many complex reservoirs used to verify the method's ability to model an arbitrarily shaped closed boundary. Specifically, the reservoir shape was a smoothed "X" measuring approximately half a mile in each "arm" from the center. A single well was placed in the bottom-left "arm", offset 1400 ft in the x and the y direction from the center. The reservoir model was verified by typecurve comparison with a numerical simulator [33,34,35,36], advanced production data analysis of rate and pressure forecasts, and confirmation of boundary dominated flow using a pure pseudo-steady state typecurve comparison.

Common reservoir properties (as described in Table 1) were used to create this model. The reservoir geometry is shown in Figure 9. The initial gas-in-place associated with this reservoir was 5.83 Bcf, with a total area of 421.4 acres. The test well was simulated at a rate of 5 Mmscf/d for a period of 8766 hours (approximately one year).

The reservoir model's constant rate dimensionless typecurve was compared with a numerical simulator and a pseudo-steady state derivative (the reserves line), as shown in Figure 10. A stronger boundary affect was observed in the numerical simulation case, beginning at approximately t_D = 1.0E6. This suggests potential problems with control points and/or image well locations in our reservoir model (further work in this area may be needed). However, the presented

model closely matched the theoretical PSS typecurve (Appendix 11), while the numerical method failed. The authors of this paper feel that honoring fully developed boundary dominated flow, and real gas behavior, is of more importance when it comes to long-term production forecasting.

Next, pressure simulation was performed to determine what affect the typecurve difference would have in practical usage. The results of the pressure simulation are shown in Figure 11. Although a variation between the numerical model and the new model presented in this paper is quite evident, it is believed this could be attributed as error to either model, as the typecurve comparison showed. Further work is needed.

Modern PDA techniques[31,32] techniques were applied to both simulations in an attempt to quantify the amount of error caused by the typecurve variations. As outlined in Appendix 11, these techniques calculate effective permeability and initial gas-in-place (Figure 12). Table 2 shows the results of the analysis. Both models provided a suitable calculation of OGIP, with the numerical simulation's OGIP being calculated high by 0.12 Bcf, and the new model's OGIP being calculated low by 0.06 Bcf. The error in back-calculated OGIP was less than 2%. The variance in permeability from the original 10 md is believed to be an affect in the production data analysis that accounts for the reservoir shape with an effective permeability. If one reviews (20) and (21) given in Appendix 11, they will notice that reservoir permeability is directly proportional to shape factor C_A. Therefore, if the wrong shape factor is used in the normalized decline procedure, then the calculated permeability is wrong. However, the combined affect remains constant during PSS.

Verification Case 3: Multiple Wells & Complex Shape. Three wells were placed in a reservoir with a non-uniform shape similar to the character "C". Well A and Well B were placed at the farthest sides of the reservoir. Well C was placed roughly between A and B (Figure 13). To demonstrate the affect adding a new well in the future would have, Well C would be shut-in for a period of the simulation and then opened to flow. The reservoir model was first verified by using typecurve comparison against the results of a numerical simulator. Further verification took place by analysis of pressure simulation results from constant rate production. Boundary dominated flow conditions were also verified with a pseudo-steady state typecurve representative of the total reservoir drainage area.

Common reservoir properties (as described in Table 1) were used to create this model. The reservoir geometry is shown in Figure 13. The initial gas-in-place associated with this reservoir was 7.05 Bcf, with a total area of 510.0 acres. Well A and Well B were produced at a constant rate of exactly 4 Mmscf/d for a period of 8766 hours (approximately 1 year). Well C recorded sandface pressures for the first 7013 hours (approximately 0.8 years) with no production. It was then produced at a constant rate of exactly 4 Mmscf/d for 1753 hours.

Typecurve comparisons (shown in Figures 14, 15, and 16) generally showed that the numerical simulator had stronger and sometimes earlier boundary affects. As with case 2, this suggests the potential for improvement by selecting new control point and/or image well locations. The presented model closely matched the pseudo-steady state typecurve, which indicates that reserves estimates should be accurate. In Well A and Well B, typecurve deviations in the numerical model were seen at approximately 6.1E8. These deviations could not be explained, but in combination with the results in case 2, there are grounds to suggest that the numerical simulator being used had stability problems during boundary-dominated flow.

Pressure simulation results were compared between the numerical simulator and the new model presented in this paper. Figure 17 shows a comparison of the sandface pressures measured at Well C. They are very closely in agreement throughout the entire simulation.

Advanced production data analysis techniques were used to determine reserves and average permeability from the flowing pressure data. Modifications to standard PDA techniques were used to analyze production data from all three wells simultaneously. The results are shown in Table 3. Both the numerical model and the new model showed close reserves matches, and a slightly lower permeability. This shows that the model is suitable for use in forecasting as it honors the correct initial gas-in-place. The lower permeability after production data analysis is attributed to the reservoir shape factor being accounted for in the calculated permeability.

Conclusions & Further Work

The following conclusions and recommendations were observed:

a) A single ring of pseudo-image wells can be used to generate no-flow boundaries for arbitrary shaped reservoirs, with multiple wells.
b) This solution is computationally more efficient than numerical simulation, or other comparable techniques such BEM.
c) The methodology presented appears to be suitable for long-term pressure and production forecasting, using pseudo-time and pseudo-pressure transformations.
d) The authors of this paper believe that this methodology may be revised for incorporation of heterogeneity. Although not presented, testing has shown that pseudo-image wells can be used to incorporate heterogeneity into existing bounded reservoir solutions.
e) Further work on pseudo image well and test point locations may improve or optimize this technology. It is possible that these can be optimized or changed in time to reduce instability.

Nomenclature

A	Reservoir Area (ft^2)
B_g	Gas FVF (Dim)
B_{gi}	Gas FVF at Initial Conditions (Dim)
C_A	Shape Factor, Dimensionless
C_n	Constant at Position/Index "n"
c_t	Total System Compressibility ($psia^{-1}$)
c_{ti}	Total System Compressibility at P_i ($psia^{-1}$)
h	Net pay (ft)
OGIP	Original-Gas-In-Place (scf)

$m(p)$	Pseudo-pressure of "P" ($psia^2/cp$)
$m(p_i)$	Pseudo-pressure of "P_i" ($psia^2/cp$)
$\Delta m(p)$	Change in Pseudo-pressure
m(p)'	Derivative of pseudo-pressure w/r ln(t)
n	Index
P	Pressure (Psia)
P_i	Initial Reservoir Pressure (psia)
P_{wf}	Flowing Sandface Pressure (psia)
p_D	Dimensionless Pressure
p_{DD}	Dimensionless Pressure Derivative w/r ln(t_D)
$p_D(s)$	Dimensionless Pressure in Laplace Space
q_g	Gas Rate at Standard Conditions (MMscf/d)
Q_g	Cumulative Gas Produced (MMscf)
s'	Wellbore Skin
s	Laplace Variable
S_{wi}	Initial Water Saturation (fraction)
t	Time (hrs)
t_a	Pseudo-time (hrs)
t_D	Dimensionless Time referenced to r_w
t_{Da}	Dimensionless Pseudo-Time referenced to r_w
t_{DA}	Dimensionless Time referenced to Area (A)
k	Permeability (md)
r_w	Wellbore radius (ft)
r_{wa}	Apparent Wellbore Radius (ft)
r_D	Dimensionless radius (Dim).
T_f	Formation Temperature (oR)
x_D	Dimensionless X-Coordinate of Well
y_D	Dimensionless Y-Coordinate of Well
x_{Do}	Dimnesionless X-Coordinate of Observation Point
y_{Do}	Dimensionless Y-Coordiante of Observation Point
γ	Euler's Constant
γ_m	Permeability Modulus
ϕ	Porosity
μ_g	Gas viscosity (cp)
μ_{gi}	Gas viscosity at P_i (cp)
σ	Stress

Subscripts:

a	Pseudo-time
A	Area
D	Dimensionless
g	Gas
i	Initial
PSS	Pseudo-steady state
t	Total
wf	Wellbore Flowing
w	Wellbore
m	Modulus

References

1. Kikani, J. "Application of Boundary Element Method to Streamline Generation and Pressure Transient Testing", Ph.D. Thesis, Stanford Univeristy, 1989.
2. ARCHER, R.A., "Computing Flow in Pressure Transients in Heterogeneous Media Using Boundary Element Methods", Ph. D Thesis, Stanford University, March 2000.
3. PECHER, R., "Boundary Element Simulation of Petroleum Reservoirs with Hydraulically Fractured Wells", Ph. Thesis, University of Calgary, 1999.
4. LIN, JER-KAUN "An Image Well Method for Bounding Arbitrary Reservoir Shapes in the Streamline Model"
5. CAUDLE, B.H., "Mechanics of Fluids in Permeable Media", Course Notes, University of Texas at Austin, 1996.
6. JANKOVIC, I., "High-Order Analytic Elements in Modeling Groundwater Flow", Ph.D Thesis, University of Minnesota, 1997.
7. HAITJEMA , "Analytical Modeling of Groundwater flow Flow", Academic Press, New York, 1995.
8. BEAR, J., "Dynamics of Fluids in Porous Media", Dover Publications Inc., New York, 1972
9. MATTHEWS,C.S., andRUSSELL, D.G.,"Pressure Buildup and Flow Tests in Wells", SPE Monograph 1, 1967.
10. EARLOUGHER, R.C., Jr., RAMEY, H.J., MILLER, F.G., and MEULLER, T.D., "Pressure Distributions in Rectangular Reserviors", J. Pet. Tech., February 1968, 199-208; Trans., AIME, 243.
11. "Gas Well Testing", 3rd Edition, ERCB Publication.
12. "Gas Well Testing: Theory & Practice", 4th Ed. Metric. Alberta Energy & Utilities Board Publication.
13. GUEVARA-JORDAN, J.M., RODRIQUEZ-HERNANDEZ, "Applications of Singular Value Decomposition to Determine Streamline Distribution for Sectionally Homogeneous Reservoirs", SPE International Symposium on Oil Field Chemistry, Texas, 19-16 February 2001. SPE Paper No. 65414
14. HONG-CHEN, L. "A Method for Bounding Irregularly-Shaped Reservoir Subject to Unsteady State Flow", Ph.D. Thesis, University of Texas at Austin, 1975.
15. Britto, P., and Sageev, A., "The Effects of Size, Shape, and Orientation of an Impermeable Region on Transient Pressure Testing", SPE California Regional Meeting, Ventura, April 8-10, 1987. SPE Paper No. 16376.
16. Second Pecher
17. Cox., D "Solution of Unsteady Flow Problems in Porous Media", PE 5980, Course Notes, Colorado School of Mines.
18. STEHFEST, H. "Numerical Inversion of Laplace Transforms", Communication of the ACM, Jan. 1970, Vol. 13, No. 1. 47-49.
19. BOURGEOIS, M., "Well Test Interpretation Using Laplace Space Typecurves", Elf Aquitaine, April 1992.
20. GRINGARTEN, A, C., RAMEY, H.J., Jr., and RAGHAVAN, R., "Unsteady-State Pressure Distributions Created by a Well With a Single Infinite-Conductivity Vertical Fracture" Soc. Pet. Eng. J. (Aug. 1974) 347-360; Trans., AIME, 257.
21. CHEN, JSIU-KUO & BINGHAM, W.E., "Pressure Buildup for a Well With Storage and Skin in a Closed Square", SPE-AIME, 44th Annual California Regional Meeting, SPE Paper No. 4890, April 4-5, 1974.
22. MATTHEWS,C.S., and RUSSELL, D.G.,"Pressure Buildup and Flow Tests in Wells", SPE Monograph 1, 1967.

23. BLASINGAME, T.A., AND LEE., W.J. "The Variable-Rate Reservoir Limits Testing of Gas Wells" SPE 17708, 1988 SPE Gas Technology Symposium.
24. MATTER, L., "Tech Talk: Pseudo-Time or Pseudo-Pressure?", Fekete Assoc. News Letter, Winter 2001.
25. AL-HUSSAINY, R, RAMEY, H.J., Jr. "Application of Real Gas Flow Theory to Well Testing and Deliverability Forecasting", JPT (196) 18, 624-636.
26. RAGHAVAN, R. "Well Test Analysis", 1993 Prentice Hall.
27. RAHAMAN, A., MATTAR, L., and ZAORAL, K., "A New Method for Computing Pseudo-Time for Real Gas Flow Using the Material Balance Equation", CIPC Annual Conference, Calgary, June 8-10, CIM Paper No 2004-182.
28. AGARWAL, R.G., "Real Gas Pseudo-time – A New Function for Pressure Buildup Analysis of MHF Gas Wells", SPE Annual ATCE , Las Vegas, Sept 23 -26. SPE Paper No. 8279.
29. van EVERDINGEN, A.F., & HURST, W., "Application of the Laplace Transformation to Flow Problems in Reservoirs", *Trans*, AIME (1949), 186, 305-24.
30. Matthews, C.S., Brons., F., and Hazebroek, P., "A Method for Determination of Average Reservoir Pressure in a Bounded Reservoir", Trans., *AIME* **201** (1954) 182-191.
31. AGARWAL, R.A., GARNDER, D.C, AND KLEINSTEIBER, S.W, "Analyzing Well Production Dada Using Combined-Type-Curve and Decline Curve Analysis Concepts", SPE 57916, 1988 SPE Annual Technical Conference and Exhibition, New Orleans, Louisiana
32. IBRAHIM, M., WATTENBARGER, R.A, AND W. HELMY "Determination of OGIP for Tight Gas Wells – New Methods", CIM 2003-012, CIPC 2003, Calgary, Alberta.
33. Z. E. Heinemann and C.W. Brand, Modeling Reservoir Geometry with Irregular Grids, paper SPE 18412 presented at 10th SPE Symposium on Reservoir Simulation, Houston, 1989.
34. C. Palagi, Generation and Application of Voronoi Grid to Model Flow in Heterogeneous Reservoirs, Ph. D., Thesis of Stanford University, 1992.
35. C. Palagi and K. Aziz, The Modeling of Vertical and Horizontal Wells with Voronoi Grid, paper SPE 24072 presented at the SPE Western Regional Meeting, Bakersfield, 1992.
36. S. Verma, Flexible Grids for Reservoir Simulation, Phd Thesis of Stanford University, 1996
37. BOURGEOIS, M. "Well Test Interpretation Using Laplace Space Typecurves", April 1992, SUPRI-D Publication, Stanford University.
38. Gardner, D.C., Hager, C.J., and Argarwal, R.G., "Incorporating Rate-Time Superposition into Decline Type Curve Analysis", SPE Paper No. 62475 prepared for presentation at the 2000 SPE Rocky Mountain Regional Meeting/ Low Permeability Reservoirs Symposium, Denver, 12-15 March.

Appendix 1 - Superposition Elements

The fact that most conintuity equations developed in fluid flow in porous media applications are linear, permits the use of a powerful tool – the principle of superposition – in solving them with or mixed, imhomogenous (linear) boundary conditions[8]. Briefly, the principle of superposition states that if p_{D1} and p_{D2} are two particular solutions of a, homogeneous linear partial differential equation, then p_{D1} and p_{D2} are also particular solutions (1) where C_1 and C_2 are constants that satisfy…..

$$p_D = C_1(p_{D1}) + C_1(p_{D2}) \quad \text{.....} \quad (1)$$

Generally, this can be expressed can be expressed as shown in (2), where the constants are adjusted so that the "new" boundary conditions are satisfied as desired. In certain cases, the sum in (2) may need to be extended to infinity in order to satisfy the desired boundary conditions.

$$p_D = \sum_{i=1}^{n} C_n(p_n) \quad \text{.....} \quad (2)$$

Appendix 2: Green's Functions

The appropriate Laplace space green's function for a cylindrical source is shown below[3,26] in (3) and assumes an unbounded infinite reservoir. In order to ensure the desired boundary condition (i.e. a no-flow boundary), the pressure gradient normal to the boundary must be equal to zero. Appendix 3 describes the calculation of the normal gradient for (3). "s" represents the Laplace parameter.

$$p_D(s) = \frac{K_0(r_D\sqrt{s})}{s^{3/2}K_1(\sqrt{s})} \quad \text{.....} \quad (3)$$

Appendix 3: Normal Derivatives

The appropriate green's function for a cylindrical source was shown earlier in (3). The derivatives of (3) with respect to x_D and y_D at an arbitrary location (i.e. an observation point on the reservoir boundary) are shown in (4) and (5). The normal derivative at some test point on boundary is given by (6). The derivation of (4) to (6) can be found in Hong-Chen[14], and other sources. Note, $r_D = (\Delta x_D^2 + \Delta y_D^2)^{1/2}$, while $\Delta x_D^2 = (x_{Do} - x_{Dw})^2$ and while $y_D^2 = (y_{Do} - y_{Dw})^2$

$$\frac{\partial[p(r_D,s)_D]}{\partial x_D} = -\frac{1}{2}\left[\frac{K_1(r_D\sqrt{s})}{r_D s}\right]\frac{2(\Delta x_D)}{K_1(\sqrt{s})} \quad \text{.....} \quad (4)$$

$$\frac{\partial[p(r_D,s)_D]}{\partial y_D} = -\frac{1}{2}\left[\frac{K_1(r_D\sqrt{s})}{r_D s}\right]\frac{2(\Delta y_D)}{K_1(\sqrt{s})} \quad \text{.....} \quad (5)$$

$$\frac{\partial[p(y_D,x_D,s)_D]}{\partial n}=\cos(\alpha)\frac{\partial[p(r_D,s)_D]}{\partial x_{Do}}+\sin(\alpha)\frac{\partial[p(r_D,s)_D]}{\partial y_{Do}} \quad \ldots (6)$$

Appendix 4: Typecurve Generation Process

In order to ensure a no-flow boundary condition, (6) must be evaluated such that $dp_D/dn = 0$ at numerous test points along the proposed boundary. The impact all pseudo image wells, and the real well must be taken into account. If one considers all real and pseudo-image wells, the normal derivative at any point on the boundary can be written as (7) shown below, where x_{Do} and y_{Do} represent observation points on the boundary. The angle (α) is the boundary angle and is measured from the positive horizontal axis to the normal line. If C_n is adjusted such that (7) is zero at all test points, then a suitable boundary condition has been met.

$$\left.\frac{\partial[p(y_D,x_D,s)_D]}{\partial n}\right|_{Real}=\sum_{n=1}^{N}C_n\left[\left[\cos(\alpha)\frac{\partial[p(x_{Do},s)_D]}{\partial x_{Do}}+\sin(\alpha)\frac{\partial[p(y_{Do},s)_D]}{\partial y_{Do}}\right]\right] \quad \ldots (7)$$

In solving (7) for C_n, an M x N results, where N represents the number of image wells, and M represents the number of test points. If there are more test points than pseudo image wells, the solution is met in an average sense and can be solved using least squares reduction or other matrix solution processes. If M = N, the solution is met exactly at the test points with little or no control at boundary positions in between the test points. During the typecurve generation process, the rate at the real well is assumed to be constant and unity. As a result, the typecurve generation process results in a constant rate solution for a single well in arbitrarly shaped reservoir.

Appendix 5: Stefhest Algorithm

The commonly known Stefhest algorithm[18] is shown below in (8) and (9). Typically, the SN is set to be in order of 12 to 18 and is even.

$$p_D(t_D)=\left(\frac{\ln(2)}{t_D}\right)\sum_{i=1}^{SN}\left[V_f(i)\,p\left(\ln(2)\frac{i}{t_D}\right)_D\right] \quad \ldots\ldots\ldots\ldots (8)$$

$$V_f(i)=\left[(-1)^{\left(\frac{SN}{2}\right)+i}\right]\sum_{k=floor\left(\frac{i+1}{2}\right)}^{\min\left(i,\frac{SN}{2}\right)}\left[\frac{k^{SN/2}(2k)!}{\left(\frac{SN}{2}-k\right)!k!(k-1)!(i-k)!(2k-i)!}\right] \quad \ldots\ldots (9)$$

Appendix 6: Semi-Log Behavior

Bourgeois[19,37] showed that if one considers a vertical well, fully completed, in a homogeneous, infinite-acting reservoir, then the asymptote for real space solution in (10) is graphically equivalent to the asymptotic Laplace space solution in (11). Specifically, plots of $p_D(t_D)$ vs. t_D and $s*p_D(s)$ vs. $1/s$ have the same asymptote behavior which is the well-known semi-log straight line. The plots in real space and Laplace space are not exactly the same, but its does imply that $p_D(s)$ can be converted to real space by simply multiply by $s = 1/t_D$ for a given $t_D = 1/s$.

$$p_D(t_D)_D=\frac{1}{2}(\ln(t_D)+2\ln(2)-\gamma) \quad \ldots\ldots\ldots\ldots (10)$$

$$s\tilde{P}(s)_D=\frac{1}{2}(\ln(\tfrac{1}{s})+2\ln(2)-2\gamma) \quad \ldots\ldots\ldots\ldots (11)$$

Appendix 7: Pressure Forecasting

Once typecurves have been generated for each well in the system, pressure profiles for multiple wells with a varying rate can easily be generated using conventional superposition methods as shown in (12). The integer "Nt" represents the current time step; "ti" represents the previous time steps; "R" represents the well of interest; and finally "NR" represents the total number of real wells in the system. Note, the dimensionless times in (12) are based upon pseudo-time (Appendix 9), not regular or real-time.

$$p(t_{D,Nt})_{D_R}=\sum_{R=1}^{NR}\sum_{ti=1}^{Nt}\left(\Delta q_{R,t}\cdot p_D(t_{Da_{NT}}-t_{Da_{ti-1}})\right) \quad \ldots (12)$$

Appendix 8: Production / Rate Forecasting

Once typecurves have been generated for each well in the system, production profiles can be generated for each well with varying specified line pressure. However, the procedure is somewhat more complicated than generating pressure profiles. Although a number of convolution and deconvolution methods were reviewed, the most effective method was found to be "back-calculating" the necessary rate at a specified time to meet the desired back pressure. As an example, (13), (14), and (15) shows the matrix formulation for the NR well case where a different backpressure has been specified for each well. Generally speaking (13), (14), and (15) is just a re-arrangement of (12) for the last unknown rate in the rate schedule. A matrix solution is required as we want to determine the rates of each well while incorporating the influence of the offset wells. The unknown rates $\Delta g_{g,n}$ can be solved using $x = A^{-1}b$.

$$A=\begin{vmatrix} p_{D,1@1}(\Delta t_D) & p_{D,2@1}(\Delta t_D) & p_{D,1NR@1}(\Delta t_D) \\ p_{D,1@2}(\Delta t_D) & p_{D,2@2}(\Delta t_D) & \cdots\cdots\; p_{D,NR@2}(\Delta t_D) \\ & \cdots\cdots & \\ p_{D,1@NR}(\Delta t_D) & p_{D,2@NR}(\Delta t_D) & p_{D,NR@NR}(\Delta t_D) \end{vmatrix} \quad \ldots (13)$$

$$b = \begin{vmatrix} p_{D,spec} - \sum_{R=1}^{NR}\sum_{ti=1}^{Nt-1}\left(\Delta q_{R,t} \cdot p_D(t_{Da_{NT}} - t_{Da_{ti-1}})\right) \\ p_{D,spec} - \sum_{R=1}^{NR}\sum_{ti=1}^{Nt-1}\left(\Delta q_{R,t} \cdot p_D(t_{Da_{NT}} - t_{Da_{ti-1}})\right) \\ .... \\ p_{D,spec} - \sum_{R=1}^{NR}\sum_{ti=1}^{Nt-1}\left(\Delta q_{R,t} \cdot p_D(t_{Da_{NT}} - t_{Da_{ti-1}})\right) \end{vmatrix} \quad \ldots (14)$$

$$x = \begin{vmatrix} \Delta q_{@1} \\ \Delta q_{@1} \\ \ldots \\ \Delta q_{@NR} \end{vmatrix} \quad \ldots\ldots (15)$$

Appendix 9: Pseudo-Time

For long-term multi-well drawdown in bounded reservoirs, the formulation of pseudo-time based upon material balance is given below in (16). As can be seen, the pseudo-time calculation requires that average reservoir pressure be determined which makes the rate prediction process in Appendix 8 iterative. Gas rates and average reservoir pressure are based on total pool production. If the cases of all wells are shut-in, then the pseudo-time [Q1,Q2,Q3Q4,Q6] calculation reverts to numerical evaluation. Note, pseudo-time is typically denoted by a subscript "a".

$$t_a(t) = (u_g c_t)_i \int_0^t \frac{\partial t}{u(\overline{P_R})c_t(\overline{P_R})} = \frac{GZ_i}{2P_i S_{gi}}\left[\frac{\overline{\Delta mp}_{01}}{q_{gt1}} + \frac{\overline{\Delta mp}_{12}}{q_{gt1}} + \ldots \frac{\overline{\Delta mp}_{n-1,n}}{q_{gtn}}\right] \quad (16)$$

Appendix 10: Pseudo-Pressure

Pseudo-pressure is commonly used in well test analysis of gas reservoirs [23,24,26,27,28]. The formulation used in this work is presented below in (17).

$$mp(p) = \frac{1}{2}\int_{pref}^{P} \frac{p}{u(p_{wf})z(p_{wf})}\partial p \quad \ldots\ldots (17)$$

Appendix 11: Pseudo-Steady State and Reserve Analysis

For long term production at a constant rate, (18) can be used to represent pseudo-steady state flow in dimensionless terms[23,24,25,26,27,28]. The Bourdet derivative associated with this equation is shown in (19).

$$p_D(t_D) = \frac{2t_D}{{r_{eD}}^2} + \ln(r_{eD}) - \frac{3}{4} \quad \ldots\ldots (18)$$

$$\frac{\partial p_D(t_D)}{\partial(\ln(t_D))} = \frac{2t_D}{{r_{eD}}^2} \quad \ldots\ldots (19)$$

Another form of pseudo-steady state analysis makes use of a plotting technique presented by Argarwal[31] et al and Gardner[38] et al to estimate OGIP. The original work uses a plot of dimensionless rate (q_D=1/p_{wD}) vs. dimensionless cumulative production (Q_{DA}) to generate the rate-cumulative-decline curve. The plot forms a straight line tending toward 1/(2π) during boundary dominated flow. The benefit of this plot is that the resulting estimate of OGIP is independent of reservoir permeability. Making use of the dimensionless definition presented by the original authors gives (20). As a modification to the original work, the y-intercept "b" was shown to be (21) and used to determine permeability of the reservoir, assuming a shape-factor of C_A of 31.62.

$$\frac{q_g}{m(p_i) - m(p_{wf})} \propto \frac{G\left[m(p_i) - m(p_r(Q_g))\right]}{m(p_i) - m(p_{wf})} + b \quad \ldots\ldots (20)$$

$$b = \frac{kh}{(1.417\times10^6)T_f\left(\frac{1}{2}\ln\left[\frac{4\cdot A}{e^{\gamma}C_A {r_w}^2}\right]\right)} \quad \ldots\ldots (21)$$

Appendix 12: Dimensionless Variable Definitions

The following definitions for dimensionless variables are used throughout this paper.

$$p_D = \frac{kh(m(p_i) - m(p_{wf}))}{1.417\cdot10^6 T_f q_g} \quad \ldots\ldots (15)$$

$$\overline{p_D} = \frac{kh(m(p_i) - m(p_R))}{1.417\cdot10^6 T_f q_g} \quad \ldots\ldots (16)$$

$$t_{AD} = \frac{0.0002637kt}{(\phi\mu_g c_t)A} \quad \ldots\ldots (17)$$

$$t_D = \frac{0.0002637kt}{(\phi\mu_g c_t){r_w}^2} \quad \ldots\ldots (18)$$

$$t_{Da} = \frac{0.0002637kt_a}{(\phi\mu_g c_t){r_w}^2} \quad \ldots\ldots (19)$$

Figure 1: Control Points and Image Wells (ft vs. ft)

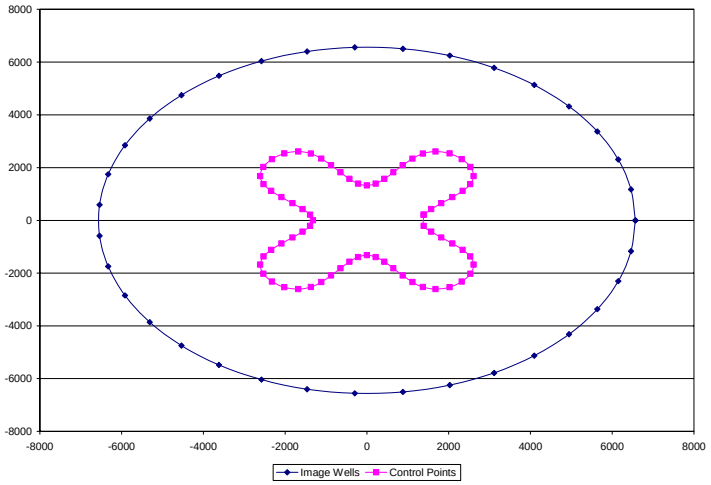

Figure 2: Stefhest vs. Approximation (p_D,p_{DD} vs. t_D)

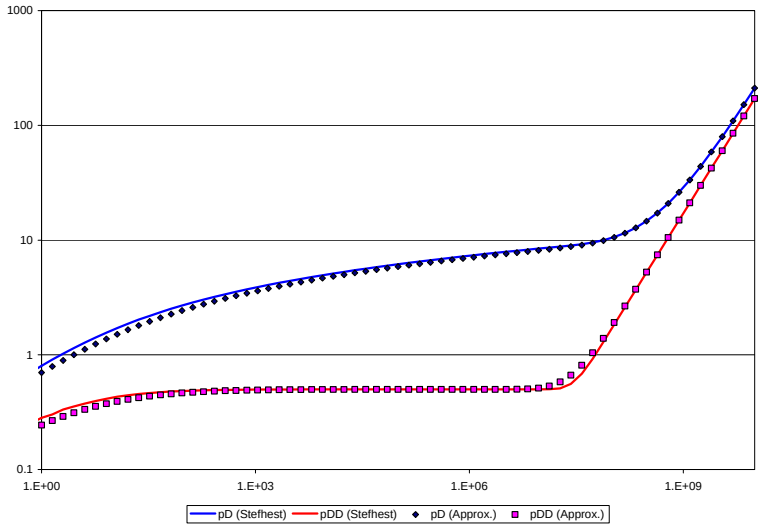

Figure 3: Desuperposition (p_D,p_{DD} vs. t_D)

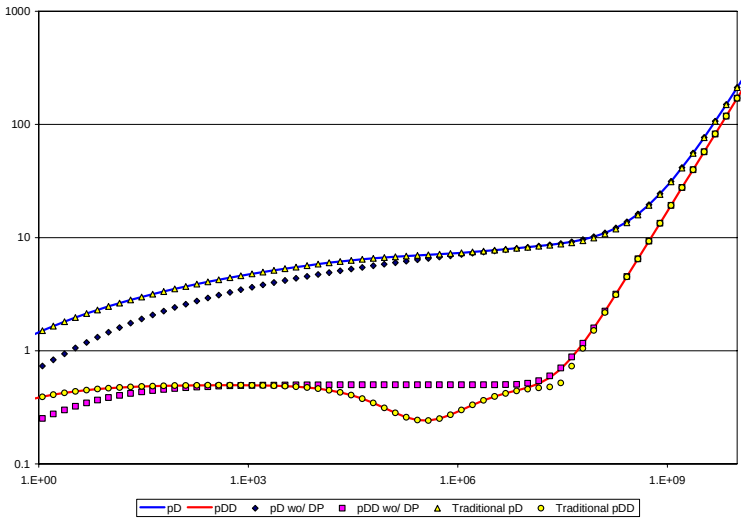

Figure 4: Effects of Real Gas Flow

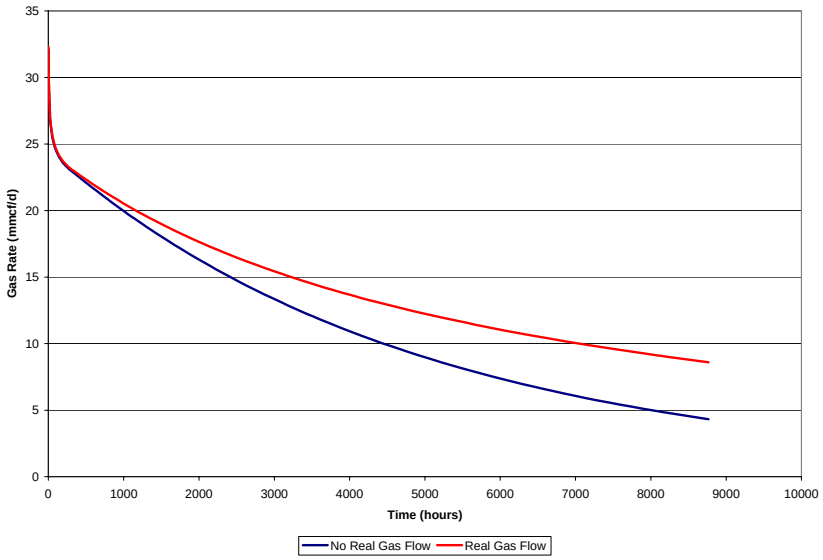

Table 1: Reservoir Properties (All Cases)

Gas Gravity	0.65	
Gas Saturation	1	(frac)
Formation Temperatrue	120	°F
Total Compressibility	1.056E-04	1/psi
Initial reservoir pressure	5000	psia
Porosity	0.1	(frac)
Net Pay	10	Feet
Wellbore radius	0.3	Feet
Permeability	10	md

Figure 5: Reservoir Geometry (Case 1)

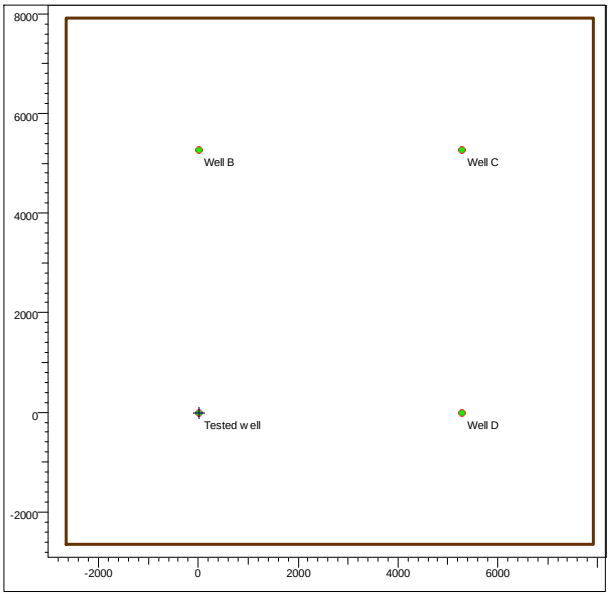

Figure 6: Typecuve For Well in 1 x 1 mile Reservoir (p_D,p_{DD} vs. t_D)

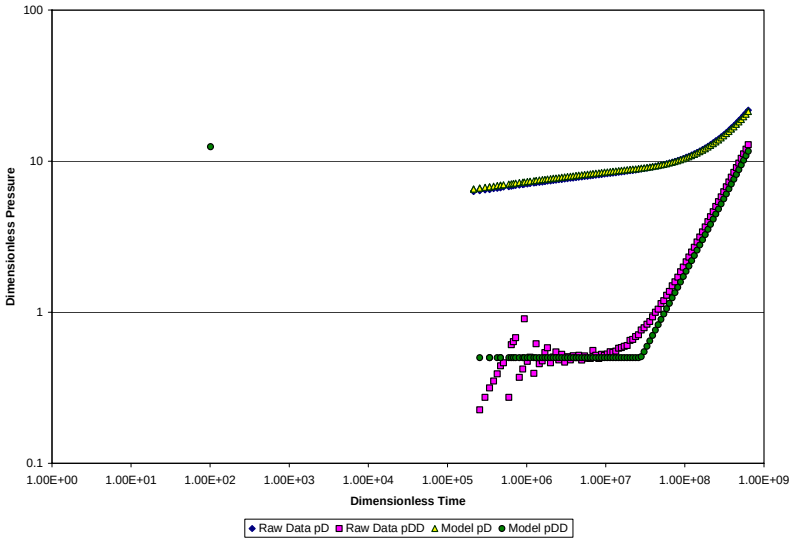

Figure 7: Typecurve Comparison (Case 1, p_D,p_{DD} vs. t_D)

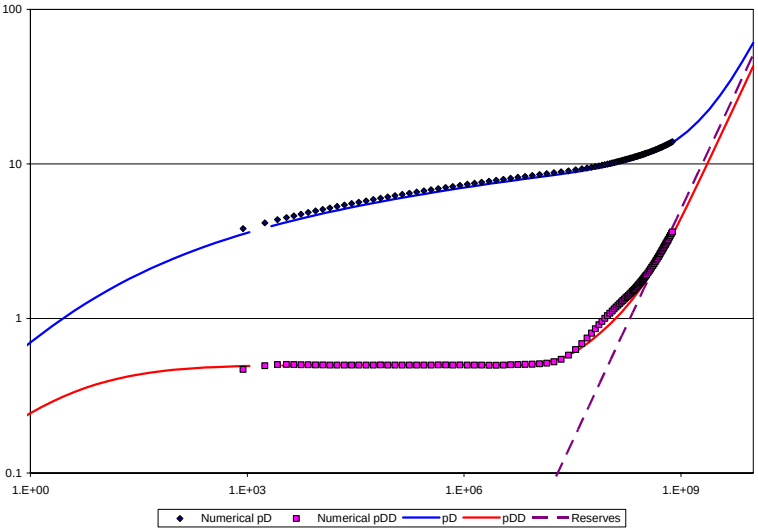

Figure 8: Pressure Simulation Match (Case 1)

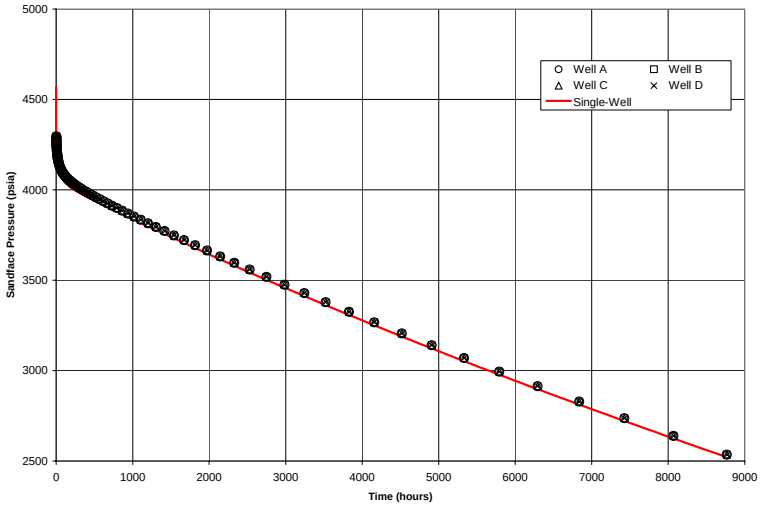

Figure 9: Reservoir Geometer (Case 2)

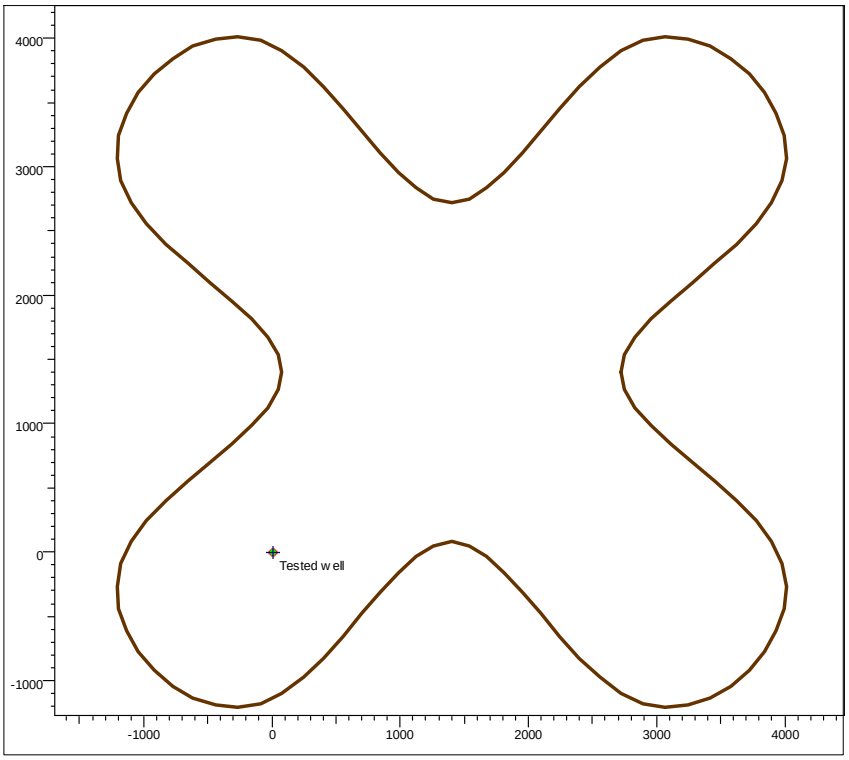

Figure 10: Typecurve Comparison (Case 2, p_D,p_{DD} vs. t_D)

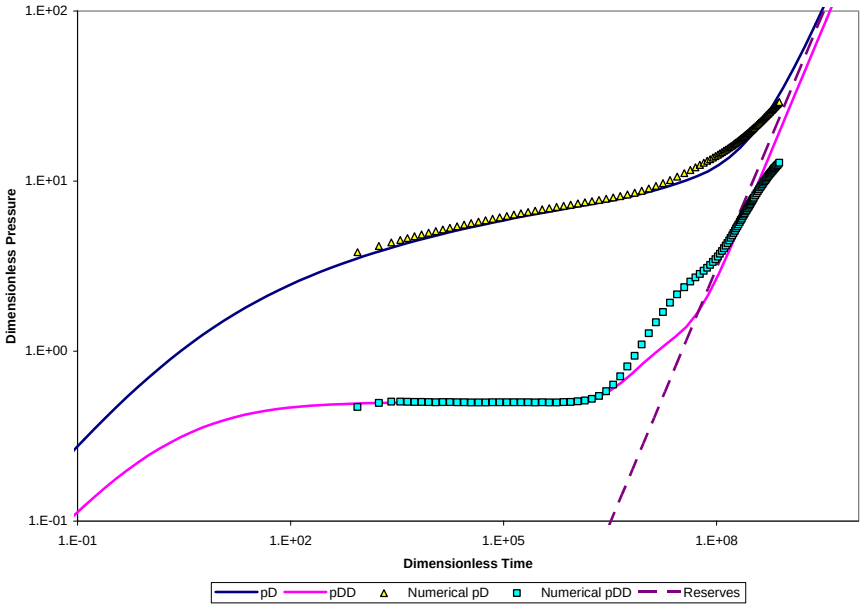

Figure 11: Pressure Simulation (Case 2)

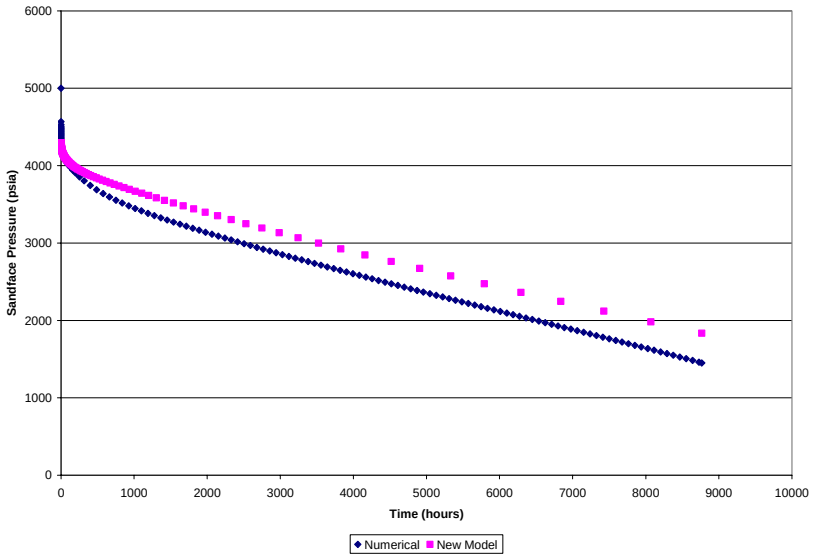

Figure 12: PDA Reserves Determination (Case 2)

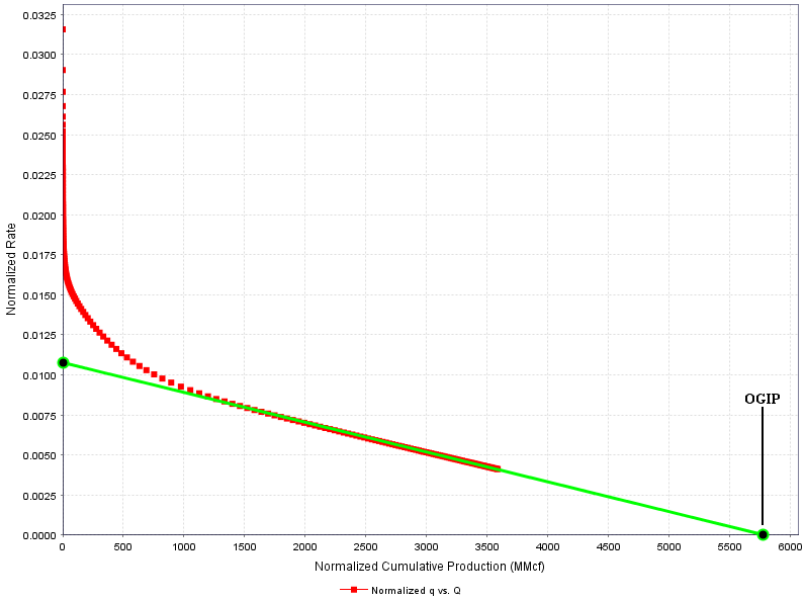

Table 2: Production Data Analysis of Pressure Simulation (Case 2)

	Permeability	Original gas-in-place
Original	10 md	5.83 Bcf
Numerical Simulation	8.9 md	5.95 Bcf
New Model	7.28 md	5.77 Bcf

Figure 13: Reservoir Geometery (Case 3)

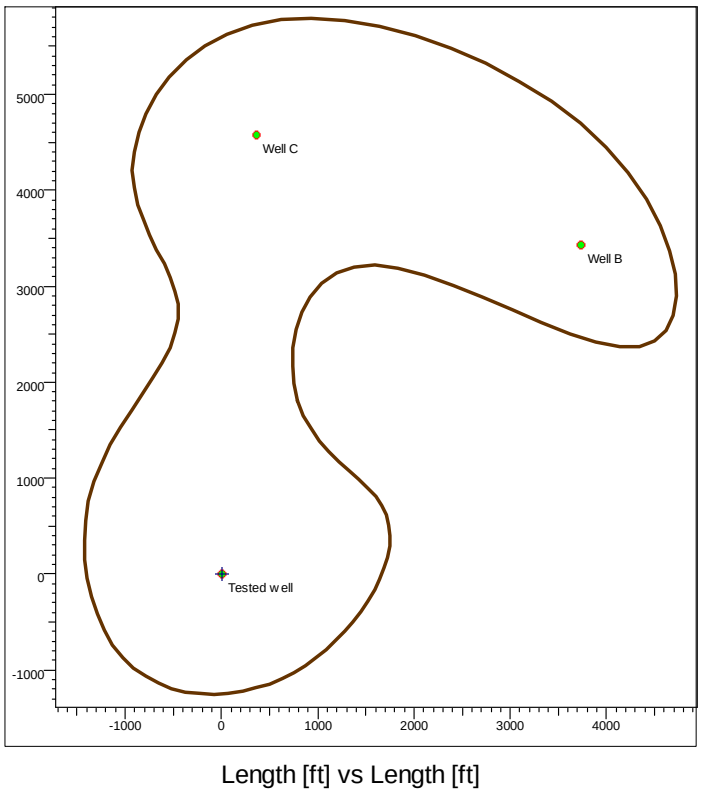

Figure 14: Typecurve Comparison of Well A (Case 3) (m(p),m(p)' vs. t)

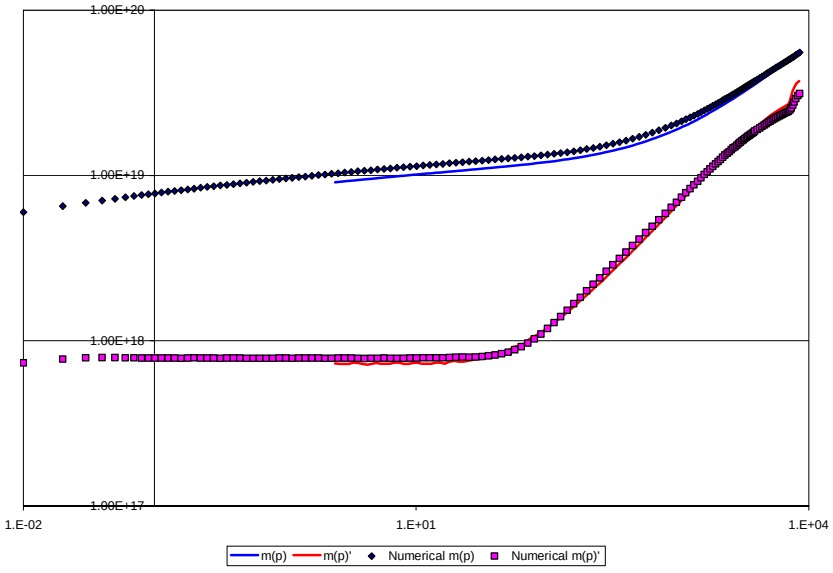

Figure 15: Typecurve Comparison of Well B (Case 3) (m(p),m(p)' vs. t)

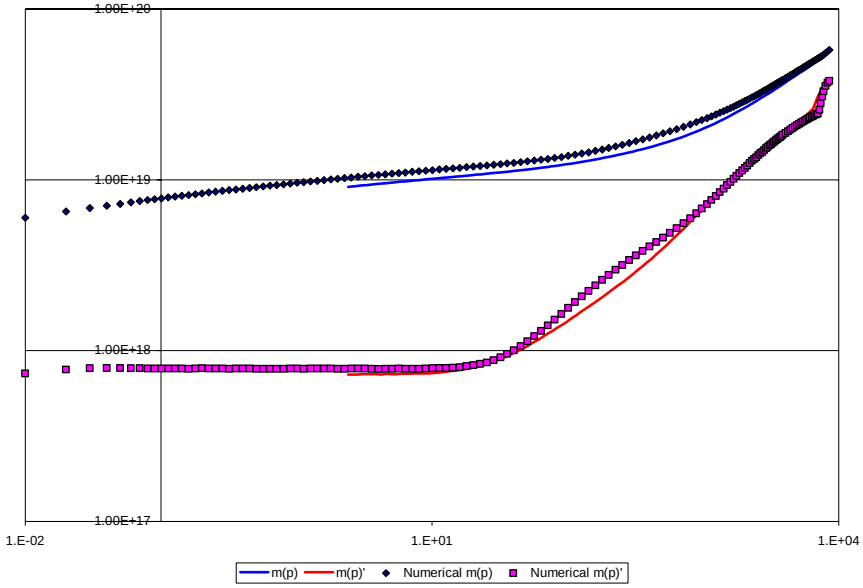

Figure 16: Typecurve Comparison of Well C (Case 3) (m(p),m(p)' vs. t)

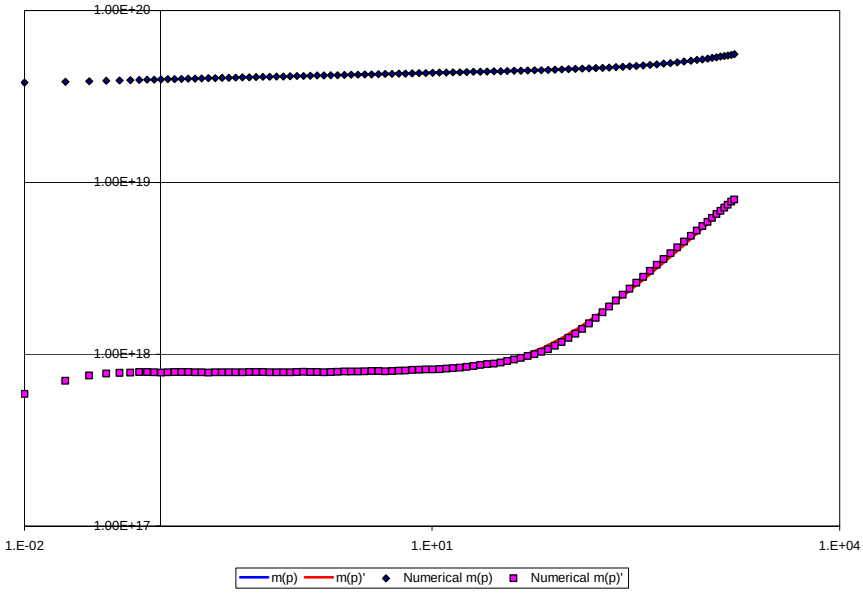

Figure 17: Pressure Simulation for Well C (Case 3)

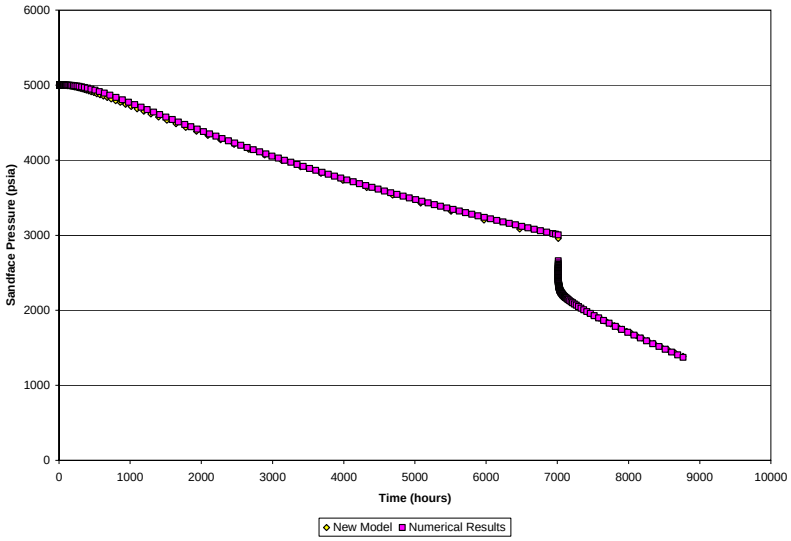

Table 3: Production Data Analysis of Pressure Simulation (Case 3)

	Permeability	Original gas-in-place
Original	10.0 md	7.05 Bcf
Numerical Simulation	8.10 md	6.88 Bcf
New Model	9.68 md	6.79 Bcf